

## Further constraints on the deep lunar interior

A. Khan and K. Mosegaard

Niels Bohr Institute, University of Copenhagen, Copenhagen, Denmark

Received 8 July 2005; revised 11 October 2005; accepted 19 October 2005; published 30 November 2005.

[1] We have inverted the most recent set of geophysical observations pertinent to lunar interior properties, including mass  $M$  and moment of inertia  $I$  as determined by Lunar Prospector, the two Love numbers  $k_2$  and  $h_2$  as well as monthly tidal dissipation  $Q$  obtained from more than 35 years of lunar laser ranging data. In wanting to assess the ability of these parameters to constrain lunar mantle and core structure, we have used a stochastically based sampling algorithm to invert the geophysical data to obtain radial density and shear wave velocity profiles. The results indicate a small liquid Fe core ( $r < 400$  km), with a shear wave velocity close to 0 km/s and a density of around 7 g/cm<sup>3</sup>. This is further corroborated by calculating the Bayes factor for the hypothesis that the lunar core is fluid against the hypothesis that it is solid, which is  $>1$ , thereby favouring the fluid core hypothesis. In addition, shear wave velocities for the lower mantle region (depths  $> 1100$  km) are generally found to be lower than upper mantle velocities and can be interpreted as implying the presence of partial melt, which can explain the unusually low lunar monthly tidal  $Q$  of  $\sim 30$ . **Citation:** Khan, A., and K. Mosegaard (2005), Further constraints on the deep lunar interior, *Geophys. Res. Lett.*, 32, L22203, doi:10.1029/2005GL023985.

### 1. Introduction

[2] The, by now, widely accepted giant impact scenario for lunar formation has the Moon forming largely out of the silicate debris that comes to lie in a circumterrestrial ring containing little iron (in comparison to bulk Earth) [Canup, 2004]. As a consequence, if a lunar Fe core is subsequently formed, it should be very small ( $<1-3\%$  by mass). What this tells us is that the possible existence of a lunar core, whatever its constitution, is an important parameter, as it holds the potential of providing key constraints on hypotheses of lunar origin and thus evolution [e.g., Canup and Richter, 2000].

[3] Over the years, beginning in the time of the Apollo era and up until very recently, the evidence based on several investigations, of geophysical as well as of geochemical nature, has converged upon the most likely existence of a small lunar Fe core [e.g., Russell et al., 1981; Hood and Jones, 1987; Mueller et al., 1988; Hood et al., 1999; Williams et al., 2001; Richter, 2002; Khan et al., 2004].

[4] Of most interest here are the analyses by Williams et al. [2001] and Khan et al. [2004]. Williams et al. [2001] claimed to determine that the present core of the Moon is liquid, contrary to many expectations. Using more than 30 years of lunar laser ranging (LLR) data, Williams et al. [2001] detected a displacement of the Moon's pole of

rotation, indicating that dissipation is acting on the rotation arising from a fluid core. Using the approximate boundary layer theory of Yoder [1995], (1-sigma) limiting radii of 352 km for a liquid Fe core and 374 km for a eutectic Fe-FeS core, respectively, were found.

[5] In wanting to assess the geophysical implications of the solution parameters determined by Williams et al. [2001], Khan et al. [2004] undertook a rigorous inversion using a Monte Carlo based sampling algorithm of the second degree lunar tidal Love number  $k_2$ , mass  $M$ , moment of inertia  $I$  and tidal dissipation factor  $Q$ . Their study, based on Bayesian hypothesis testing, used the data to distinguish between two competing hypotheses concerning core state, size and constitution. One hypothesis had the Moon containing a liquid core whereas the other one considered the core to be solid, with no bounds put on either size or composition (density). Their results indicated that a liquid Fe core with a density of  $\sim 7$  g/cm<sup>3</sup> and a radius of about 350 km was the most likely solution.

[6] In the present study we shall continue along the lines of Khan et al. [2004], that is, by inverting a set of geophysical solution parameters in order to further constrain the deeper structure of the Moon. The approach taken here distinguishes itself from the one by Khan et al. [2004] in that, 1) we have added the information provided by the second degree displacement Love number  $h_2$ , measuring the vertical displacement of the lunar surface, which is sensed by the laser ranges as the Moon flexes due to the varying tides [Williams et al., 2005] and 2) no prior assumptions are presently invoked about the state of the core as in the study of Khan et al. [2004], meaning that all possible combinations of core state, size and composition are equally probable and that only data are used to constrain the outcome.

### 2. Method of Analysis

[7] The specific goal of the present study is to infer information about the lunar radial  $S$ -wave velocity  $v_S(r)$  and density profile  $\rho(r)$  by inverting the second degree tidal Love number  $k_2$ , displacement Love number  $h_2$ , global monthly tidal dissipation  $Q$ , mass  $M$  and moment of inertia  $I$ . The measured values are  $k_2 = 0.0227 \pm 0.0025$ ,  $h_2 = 0.045 \pm 0.01$ ,  $Q = 30 \pm 4$  [Williams et al., 2005],  $M = 73.477 \pm 0.033 \times 10^{22}$  kg and  $I/MR^2 = 0.3935 \pm 0.0002$  [Konopliv et al., 2001; M. A. Wiczeorek, personal communication, 2004], where  $R$  is the mean radius of 1737.1 km [Smith et al., 1997].

[8] Our model of the Moon is assumed to be spherically symmetric and divided into 5 shells of variable thickness. In addition to layer thickness  $d$ , each shell is described by shear modulus  $\mu$ , bulk modulus  $\kappa$ , density  $\rho$  and local dissipation  $q$ , resulting in a 25-dimensional model space. The parametrisation of our model into 5 layers follows the

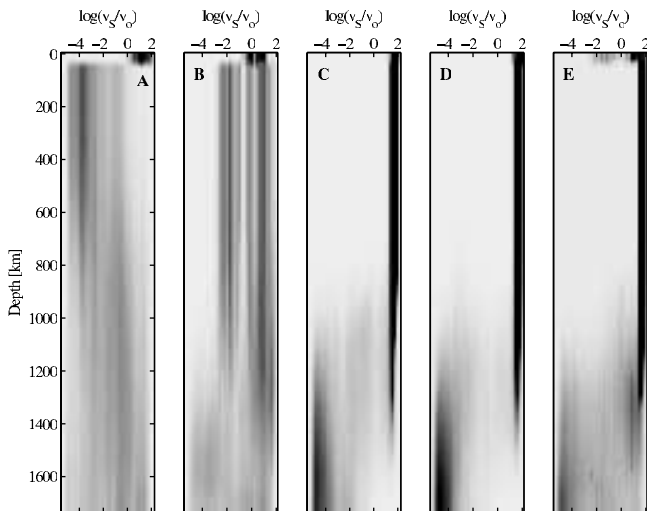


**Figure 1.** Sampled 1D marginal prior and posterior  $S$ -wave velocity models depicted using  $\log(v_s/v_o)$ , where  $v_o = 1$  km/s. The five figures are obtained by sequential analysis of the data set. A. prior information, B. inversion of only  $M$  and  $I$ , C. inversion of only  $k_2$ , D. inversion of only  $h_2$  and E. joint inversion of all data. The figures have been put together by analysing sampled  $S$ -wave velocities at every kilometer and then combining these to produce radial profiles. The different shades of gray are directly related to the probability of occurrence with black as most probable and white as least probable. Focusing on sampled prior information in the central region (near-homogeneous), the chosen parametrisation is seen to concentrate, a priori, a significant part of the probability mass at low  $S$ -wave velocities. However, as is apparent in E, data translate (constrain) an even larger part of the probability mass to very low velocities, signaling data sensitivity in this region.

general division of the lunar interior into crust, upper, middle and lower mantle as well as a core. All sampled models are models with relatively high likelihood values that fit data within uncertainties, thereby allowing a sufficient sampling of the posterior distribution. A model containing more layers could obviously also have been chosen, although at the expense of increasing model solution complexity. Given radial profiles of these parameters we can calculate model values of  $k_2$ ,  $h_2$ ,  $Q$ ,  $M$  and  $I$ . Estimating Love numbers for a given model of  $\mu$ ,  $\kappa$  and  $\rho$  is done by solving six linear differential equations using appropriate boundary conditions [Alterman *et al.*, 1959]

$$\frac{dy_i^n}{dr} = \Omega_{ij} y_j^n \quad i, j = 1, \dots, 6. \quad (1)$$

where the  $y_i^n$ 's correspond to harmonic deformations of degree  $n$  and the  $\Omega_{ij}$ 's are functions of the rheological parameters, harmonic degree and frequency of the deformation. Love numbers of degree  $n$  are then  $h_n = y_1^n$ ,  $l_n = y_3^n$ ,  $k_n = y_5^n$ . Global tidal dissipation is calculated using  $Q^{-1} = \text{Im}(k_2)/\text{Re}(k_2)$ , whereas  $M$  and  $I$  are easily evaluated by simple integration of the density profile.

[9] The stochastic sampling algorithm operates by sampling solutions to the inverse problem that fit the

observed data within their error bars and at the same time satisfies known or assumed physical a priori constraints. We have used a Markov chain Monte Carlo (MCMC) method designed to sample the model parameter space according to the posterior probability density (posterior  $pd$ ), which is mathematically given by the conjunction of the various probability density functions ( $pdf$ ), describing prior information, data uncertainties and the physical laws governing the relationship between data and model parameters [e.g., Mosegaard and Tarantola, 1995; Mosegaard, 1998].

[10] As the results are conditioned on data and any prior assumptions made, let us briefly enumerate these (for details see Khan *et al.*, 2004). Except for the crustal layer, the physical extent of a given shell  $d_i$ , defined by the radii of the layer boundaries  $r_i$  and  $r_{i+1}$  can assume any value within the confines of the boundaries ultimately above and below the boundary under consideration, while lunar surface and center are anchored at  $r = 1737$  km and 0 km, respectively. As the data studied here are not really sensitive to crustal structure, we constrained crustal thickness to vary between 30 and 60 km depth. The parameters  $\mu$ ,  $\kappa$ ,  $\rho$  and  $q$  are parametrised using their logarithms and these are assumed to be uniformly distributed within some large intervals, corresponding to  $\rho$  varying from 3 to 7.5 g/cm<sup>3</sup>,  $q$  from 1 to 200 and  $v_s$  from 0.001 to 10 km/s. In addition we are only interested in sampling density models that increase with depth and thus require that  $\rho$  satisfy the sequence  $\dots \rho_{i-1} \leq \rho_i \leq \rho_{i+1} \dots$ . As concerns data distribution, we assume these to be individually independent and described using gaussian uncertainties, resulting in a likelihood function of the form

$$\mathcal{L}(\mathbf{m}) \propto \prod_j \exp \left\{ -\frac{[d_{obs}^j - d_{cal}^j(\mathbf{m})]^2}{2\sigma_j^2} \right\} \quad (2)$$

where  $d_{obs}$  denotes observed data,  $d_{cal}(\mathbf{m})$  synthetic data computed using model  $\mathbf{m}$  with  $j$  alluding to the particular

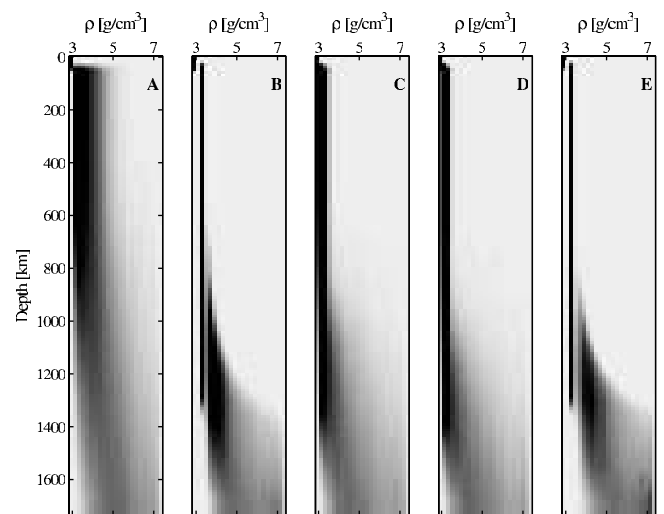


**Figure 2.** Sampled prior and posterior  $\rho$  models depicted in the form of 1D marginals. The five figures are, as in Figure 1, obtained by sequential analysis of the data set. A. prior information, B. inversion of only  $M$  and  $I$ , C. inversion of only  $k_2$ , D. inversion of only  $h_2$  and E. joint inversion of all data. Shades of gray as in Figure 1.

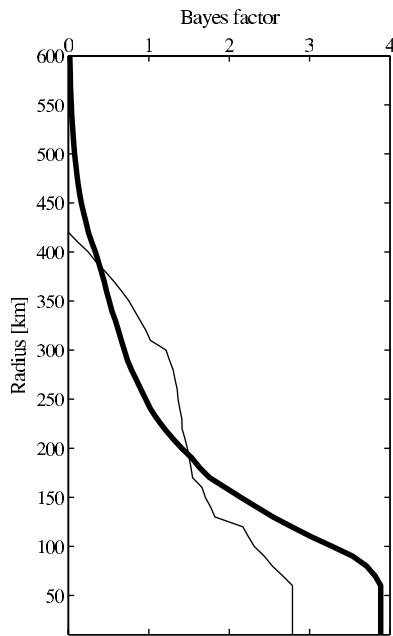


**Figure 3.** The Bayes factor as a function of radius for two different hypothesis tests. The first test (thick line) aimed at distinguishing between a fluid (hypothesis 1:  $v_S < 0.5$  km/s) and a solid core (hypothesis 2:  $v_S > 3.5$  km/s). The second test (thin line) measured the relative importance of a high density core (hypothesis 1:  $\rho > 7$  g/cm<sup>3</sup>) versus a core made of troilite (hypothesis 2:  $\rho \in [5.1; 5.3]$  g/cm<sup>3</sup>). In both cases  $B_{ij} > 1$  for the central region, implying that a small high density fluid core is favoured by data.

geophysical observation and  $\sigma$  is the uncertainty on either of these.

### 3. Results and Discussion

[11] In order to provide the reader with a sense of the resolution, that is, how well the model parameters are resolved from data, we have displayed prior next to posterior as a direct comparison reflects how much information is contained in the data. Furthermore, to address the question of resolution, which from our point of view amounts to asking what sort of information is actually contained in the individual data and moreover how much can these individually resolve, we have split up the data and inverted these separately. In displaying the results we therefore show prior and several posteriors, including those obtained from an inversion of 1. only  $M$  and  $I$ , 2. only  $k_2$ , 3. only  $h_2$  and finally 4. all data. Figures 1 and 2 display marginal 1D prior and posterior  $pd$ 's depicting the radial variation of sampled  $v_S$  and  $\rho$  models. What can be extracted from Figures 1 and 2 is the probability for obtaining certain model parameter values at a given depth. The sequential analysis of the data nicely portrays the increased amount of information obtained as we add more data in the inversion. Most importantly, data are seen to constrain the deep structure. For the central part of the Moon the most probable shear wave velocity is  $\sim 0$  km/s, while density is  $\sim 7$  g/cm<sup>3</sup>. Figure 1 shows that the fluid core conclusion is largely based on the LLR data. These results are in line with earlier

results and interpretations, as discussed in the introduction, of a small liquid Fe core. Concerning solid cores, these are seen to be much less probable than their liquid counterpart, which, it should be reminded is not because of prior restrictions as  $S$ -wave velocities up to 10 km/s are allowed. Thus, the fact that models with solid cores are less probable is related to data, since neither prior information nor physical theory preclude such models from being sampled. The solid-body part of the mantle (upper and middle mantle), down to a depth of roughly 1100 km, is preferentially characterised by  $S$ -wave velocities of  $\sim 4.5$  km/s and densities of  $\sim 3.3$  g/cm<sup>3</sup>, also in agreement with our earlier results. For the lower mantle most probable solutions seem to imply lower velocities than the upper mantle, also in accordance with our derivations. Furthermore, for the lower mantle the solution is in-between the values obtained in the layers above and below and is presently interpreted as implying the presence of partially molten material. This interpretation is in line with inferences drawn from the analysis of the Apollo lunar seismic data which led Nakamura *et al.* [1973] to postulate the possible existence of a region of partial melt constituting the lower mantle. Further evidence for the presence of a partially molten region, although indirect, also comes from the low monthly  $Q$ . As noted by Williams *et al.* [2001] the monthly  $Q$  of the Moon is surprisingly low by terrestrial standards and could possibly be explained as being due to the presence of an attenuating zone.

[12] As numerical modeling experiments usually require a minimum number of assumptions, the results are of course to be viewed in the light of these. This is especially true when having to draw inferences from inverse calculations. The approach adopted here was to assume as few prior constraints as possible on model parameters and to let data be the constraining factor. This is reflected in the broad homogeneous prior  $pd$ 's used here. Should it happen that data cannot constrain the model parameters to any appreciable degree, because of a lack of information, i.e. excessively large error bars, then the posterior  $pd$ 's will resemble the prior  $pd$ 's. This is seen not to be the case for any of the layers considered here, implying that data are indeed able to provide information on mantle as well as core structure (see Figure 1 for further discussion). Also, as we have made the assumption of spherical symmetry, effects of asymmetrical contributions to data are not accounted for.

[13] In wanting to quantitatively assess our results concerning the core we use the standard Bayesian approach to hypothesis testing in the form of the Bayes factor, which is a summary of the evidence for one hypothesis against another one. The Bayes factor  $B_{ij}$  for model  $M_i$  against model  $M_j$  given data and prior information is defined as the ratio of posterior to prior odds, or equivalently as the ratio of likelihoods, signaling the effect of data on changing relative prior beliefs into relative posterior beliefs [e.g., Khan and Mosegaard, 2002]

$$B_{ij} = \frac{\mathcal{L}(M_i)}{\mathcal{L}(M_j)}$$

Figure 3 shows the results for two such hypothesis tests where we tested for most probable core state and density. As  $B_{ij} > 1$  for both tests in the central region, the low velocity

nature of the core ( $v_S \sim 0$  km/s) as well as its high density ( $\rho \sim 7$  g/cm<sup>3</sup>) are to be considered as most likely results.

[14] Ongoing analyses of LLR data [Williams *et al.*, 2005] have strengthened the case for a fluid core. As discussed in detail by Williams *et al.* [2005], the variations in lunar rotation and orientation measured by LLR are sensitive to a number of effects, including tidal Love number  $k_2$ , solid-body tidal dissipation and dissipation at the fluid-core/solid-mantle boundary. Core-mantle boundary (CMB) flattening and fluid core moment of inertia are less well sensed. The interpretation of the dissipation results invoked both strong tidal dissipation and interaction at the CMB. The LLR determined value of  $k_2$  has decreased from previous estimates which were based on a spherical core and from the value determined due to the fact that core oblateness has been taken into account (larger core oblateness results in a smaller  $k_2$ ). Spacecraft-determined tidal variation of the gravity field gives a value of  $k_2 = 0.026 \pm 0.003$  [Konopliv *et al.*, 2001]. Independent evidence for a liquid core would stem from the detection of any oblateness of the CMB as it should influence the tilt of the lunar equator to the ecliptic plane [Dickey *et al.*, 1994]. Core oblateness depends on the fluid core moment and the CMB flattening. Recent progress in the determination of CMB flattening has improved and now seems significant, which together with the present results strengthens the case for a fluid core. Finally, a solid inner core existing inside the fluid core might also be a distinct possibility. However, the current analysis is not able to detect it and we have to rely on future measurements to reveal any gravitational interactions between it and the mantle.

[15] **Acknowledgments.** We are grateful to J. G. Williams for valuable comments throughout this study. Constructive comments by two anonymous reviewers also improved the manuscript. A. Khan acknowledges financial support from the Carlsberg foundation.

## References

- Alterman, Z., H. Jarosch, and C. L. Pekeris (1959), Oscillations of the Earth, *Proc. R. Soc. London, Ser. A*, 252, 80.
- Canup, R. M. (2004), Simulations of a late lunar forming impact, *Icarus*, 168, 433.
- Canup, R. M., and K. Righter (2000), *Origin of the Earth and Moon*, edited by R. M. Canup and K. Righter, p. 397, Arizona Univ. Press, Tucson.
- Dickey, J. O., et al. (1994), Lunar laser ranging: A continuing legacy of the Apollo program, *Science*, 265, 482.
- Hood, L. L., and J. H. Jones (1987), Geophysical constraints on lunar bulk composition and structure: A reassessment, *J. Geophys. Res.*, 92, 396.
- Hood, L. L., D. L. Mitchell, R. P. Lin, M. H. Acuna, and A. B. Binder (1999), Initial measurements of the lunar-induced magnetic dipole moment using lunar prospector magnetometer data, *Geophys. Res. Lett.*, 26, 2327.
- Khan, A., and K. Mosegaard (2002), An inquiry into the lunar interior: A non-linear inversion of the Apollo lunar seismic data, *J. Geophys. Res.*, 107(E6), 5036, doi:10.1029/2001JE001658.
- Khan, A., K. Mosegaard, J. G. Williams, and P. Lognonné (2004), Does the Moon possess a molten core?: Probing the deep lunar interior using results from LLR and Lunar Prospector, *J. Geophys. Res.*, 109, E09007, doi:10.1029/2004JE002294.
- Konopliv, A., A. B. Binder, L. L. Hood, A. B. Kucinskis, W. L. Sjogren, and J. G. Williams (1998), Improved gravity field of the Moon from Lunar Prospector, *Science*, 281, 1476.
- Konopliv, A. S., S. W. Asmar, E. Carranza, W. L. Sjogren, and D. N. Yuan (2001), Recent gravity models as a result of the Lunar Prospector Mission, *Icarus*, 150, 1.
- Mosegaard, K. (1998), Resolution analysis of general inverse problems through inverse Monte Carlo sampling, *Inverse Probl.*, 14, 405.
- Mosegaard, K., and A. Tarantola (1995), Monte Carlo sampling of solutions to inverse problems, *J. Geophys. Res.*, 100, 12,431.
- Mueller, S., G. J. Taylor, and R. J. Phillips (1988), Lunar composition: A geophysical and petrological synthesis, *J. Geophys. Res.*, 93, 6338.
- Nakamura, Y., D. Lammlein, G. V. Latham, M. Ewing, J. Dorman, F. Press, and M. N. Toksöz (1973), New seismic data on the state of the deep lunar interior, *Science*, 181, 49.
- Righter, K. (2002), Does the Moon have a metallic core? Constraints from giant-impact modelling and siderophile elements, *Icarus*, 158, 1.
- Russell, C. T., P. J. Coleman Jr., and B. E. Goldstein (1981), Measurements of the lunar induced magnetic moment in the geomagnetic tail: Evidence for a lunar core, *Proc. Lunar Planet. Sci. Conf.*, 12th, 831.
- Smith, D. E., M. T. Zuber, G. A. Neumann, and F. G. Lemoine (1997), Topography of the Moon from the Clementine LIDAR, *J. Geophys. Res.*, 102, 1591.
- Williams, J. G., D. H. Boggs, C. F. Yoder, J. T. Radcliff, and J. O. Dickey (2001), Lunar rotational dissipation in solid body and molten core, *J. Geophys. Res.*, 106, 27,933.
- Williams, J. G., D. H. Boggs, and J. T. Radcliff (2005), Lunar fluid core and solid-body tides, *Lunar Planet. Sci.*, XXXVI, abstract 1503.
- Yoder, C. F. (1995), Venus' free obliquity, *Icarus*, 117, 250.

A. Khan and K. Mosegaard, Niels Bohr Institute, University of Copenhagen, Juliane Maries Vej 30, DK-2100 Copenhagen Oe, Denmark. (amir@gfy.ku.dk; klaus@gfy.ku.dk)